4. Water and salt balances at farmer fields

R. Singh, J.C. van Dam and R.K. Jhorar

Abstract

Experiments in combination with deterministic simulation models offer the opportunity to gain detailed insights into the system behaviour in space and time. In this chapter the agrohydrological model SWAP is used to analyse the water flow and salt transport at the measured farmer fields. The soil textures range from clay loam to loamy sand. The percentages of canal water with respect to total amount of irrigation water range from 30 to 90%. Most of the information required to apply SWAP could be measured directly in the field or laboratory. The main unknowns were the soil hydraulic functions which are valid at field scale level. These functions were determined by automatic calibration with PEST using measured soil moisture and salinity profiles before and after irrigations. The calibrated SWAP model was used to derive the water and salt balances. In case of the wheat-cotton rotation, the relative transpiration of wheat was in general ≈0.68, which means moderate water stress. An exception were fields in saline groundwater areas which showed more stress (≈0.35). The cotton crops at all fields showed a relative transpiration ≈0.60, which is caused by irrigation water shortage and low rainfall in the monsoon of 2002. In case of the wheat-rice rotation, the relative transpiration of both wheat and rice are close to potential levels. This is attributed to the availability of sufficient tube well water with good quality. Pedotransfer functions based on the soil database HYPRESS were used to derive soil hydraulic functions for the farmer fields and next simulate the water and salt balance. In comparison with the results of the calibrated SWAP, soil hydraulic fucntions based on pedotransfer functions resulted in almost similar relative transpirations. This means that pedotransfer functions might be used in the regional analysis to derive soil hydraulic functions for water productivity analysis.

4.1 Introduction

Climate, soil, and regional groundwater flow are natural factors which affect local and regional soil water flow and salt transport. Besides these natural factors, there are certain man-made factors like cropping pattern, irrigation and groundwater exploitation. Unfortunately, the combination of these natural and man-made factors in Sirsa Irrigation Circle (SIC) have resulted in unfavourable environmental conditions. For instance during October 1998 about 13% of the SIC area experienced waterlogging (groundwater depth < 3 m) and salinization (*Singh*, 2000a). At the same time with present irrigation efficiencies there is not enough rain and canal water available to meet the crop water demands (*Dhindwal and Kumar*, 2000). Since it is hardly possible to withdraw more water from natural resources, future irrigation developments should focus on improvement of water use efficiency at both field and regional scale. Measures which may improve the water productivity concern e.g. the irrigation schedulling, the cropping pattern, or conjunctive use of good quality canal water and bad quality groundwater. The key to evaluate different options lies in the assessment of the resulting water and salt balances (*Bastiaanssen et al.,* 1996).

Field experiments yield site-specific information and are very expensive and time consuming to conduct for all crop growth conditions, especially if they should be representative for a sequence of years. However experiments in combination with deterministic simulation models offer the opportunity to gain detailed insights into the system behaviour in space and time (*Perreira et al.*, 1992; *Roest et al.*, 1993). Deterministic soil and water balance models like SWAP quantify all water and salt balance components and their interactions in the Soil-Water-Plant- Atmosphere continuum during the whole year. The accuracy of these predictive models depends upon proper identification of the required model input parameters. Before application of these models in a certain situation, a profound analysis of its input parameters and their influence on the predicted results is necessary. Some of the model input parameters can be measured directly in the field, but others remain uncertain. Inverse modeling can be used to determine indirectly the remaining unknown input parameters. In order to apply inverse modeling, accurate field observations are needed which characterize the system behaviour and the uncertain parameters should be sufficiently sensitive to the field observations.

The main objective of this chapter is to evaluate the present agricultural practices with respect to the field scale water and salt balance. In order to do so Water Management Response Indicators (WMRI) are defined which relate different water and salt balance components (*Bastiaanssen et al.*, 1996). The agrohydrological model SWAP was calibrated using measurements at farmer fields for various combinations of soil, crop, irrigation amount, water quality and groundwater level. Subsequently the calibrated model was used to analyse the effect of viable options for efficient and sustainable water management.

4.2 SWAP model description

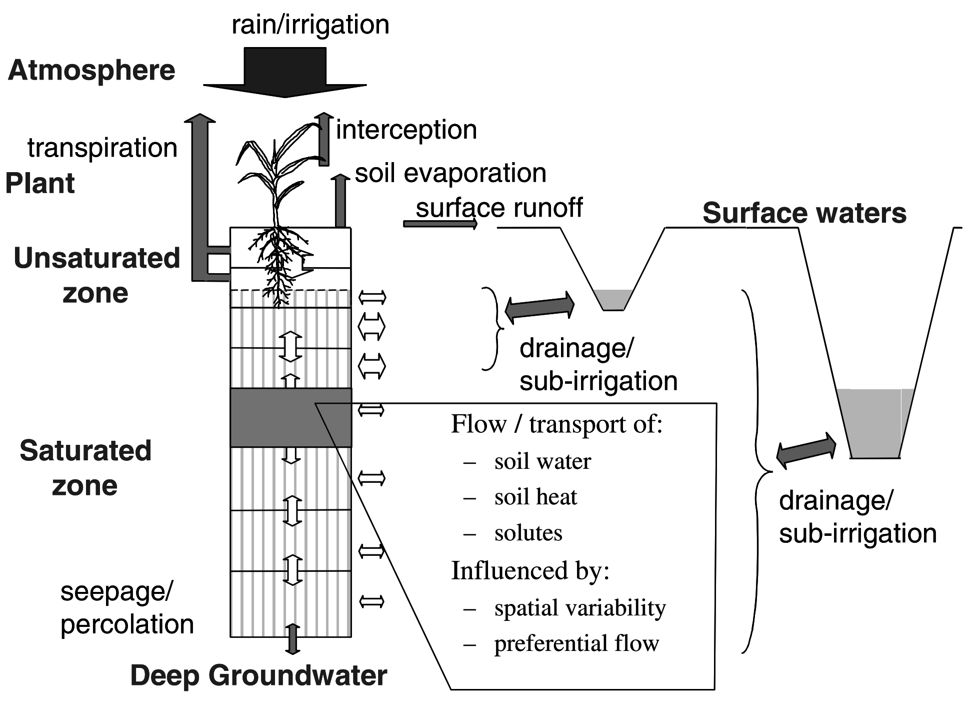

Figure 4.1 Schematization of hydrological processes incorporated in SWAP.

SWAP (*Van Dam et al.,* 1997; *Kroes et al.*, 1999) is an agrohydrological model (Soil-Water-Atmosphere-Plant) which calculates water and salt balances of cropped soil columns. Using deterministic, physical laws, SWAP simulates variably saturated water flow, solute transport and heat flow in top soils in relation to crop development (Fig. 4.1). SWAP offers a wide range of possibilities to address practical questions in the field of agricultural water management and environmental protection. Options exist for irrigation scheduling, drainage design, salinity management, leaching of solutes and pesticides, and crop growth.

SWAP may simulate up to three crops in a year and contains a detailed (Chapter 5) and simple crop model. For calibration of water flow and salt transport at farmer fields, the simple crop model was used. In this model the leaf area index, crop height and rooting depth are prescribed as function of crop development stage, which is either controlled by the temperature sum or linear in time. These measured data are sufficient to determine rainfall interception, potential soil evaporation and crop transpiration at the top boundary. When the simple crop model is used, the effect of water and salt stress on crop production might be quantified with yield response factors as function of crop development stage (*Doorenbos and Kassam*, 1979; *Smith*, 1992):

$$1-\frac{Y_{\mathrm{a},k}}{Y_{\mathrm{p},k}}=K_{\mathrm{y},k}\left(1-\frac{T_{\mathrm{a},k}}{T_{\mathrm{p},k}}\right) \tag{4.1}$$

where $Y_{\mathrm{a},k}$ and $Y_{\mathrm{p},k}$ ($\mathrm{ML^{-3}}$) are the actual and potential crop yield during growing stage k, $T_{\mathrm{a},k}$ and $T_{\mathrm{p},k}$ (L) are the actual and potential transpiration during growing stage k, and $K_{\mathrm{y},k}$ (-) is the yield response factor. For semi-arid and arid regions, a simplified linear relationship between relative yield, Y_a / Y_p and relative transpiration, T_a / T_p might be applied (*de Wit*, 1958; *Hanks*, 1974, 1983; *Stewart et al.*, 1977; *Feddes*, 1985):

$$\frac{Y_\mathrm{a}}{Y_\mathrm{p}}=\frac{T_\mathrm{a}}{T_\mathrm{p}} \tag{4.2}$$

4.2.1 Water and salt balance

The water balance (cm) of a vertical soil column with vegetation during a certain period can be written as:

$$\Delta W = P + I - R - P_\mathrm{i} - T_\mathrm{a} - E_\mathrm{a} - E_\mathrm{w} + Q_\mathrm{bot} \tag{4.3}$$

where ΔW is the change in soil water storage, P is precipitation, I is irrigation, R is surface runoff, P_i is interception by vegetation, T_a is actual transpiration, E_a is actual soil evaporation, E_w is evaporation of ponding water and Q_bot is water percolation at the soil column bottom (+ upward).

The salt balance of this soil column over a certain time interval can be written as:

$$\Delta C = PC_\mathrm{p} + IC_\mathrm{i} + Q_\mathrm{bot}C_\mathrm{bot} \tag{4.4}$$

where ΔC is the change in salt storage (g $\mathrm{cm^{-2}}$), C is solute concentration (g $\mathrm{cm^{-3}}$), and subscripts *p*, *i*, and *bot* refer to precipitation, irrigation and bottom flux, respectively.

4.2.2 Soil water flow

Soil water movement is governed by the gradient of the hydraulic head, H (cm) which be written as:

$$H = h + z \tag{4.5}$$

where h is the soil water pressure head (cm) and z is the vertical coordinate (+upward). In unsaturated soils water flow is predominantly vertical. Using Darcy’s law, the water flux density q (cm $\mathrm{d^{-1}}$) can be expressed as (+ upward):

$$q=-K\left(h\right)\left[\frac{\partial h}{\partial z}+1\right] \tag{4.6}$$

where K is the unsaturated hydraulic conductivity (cm $\mathrm{d^{-1}}$) as function of soil water pressure head. The law of mass conservation of a soil column with root water extraction S_a ($\mathrm{d^{-1}}$) gives:

$$\frac{\partial\theta}{\partial t} = -\frac{\partial q}{\partial z} - S_a(z) \tag{4.7}$$

where θ is the volumetric soil water content ($cm^3\ cm^{-3}$) and t is time (d). Combination of Eqs. 4.6 and 4.7 yield the general soil water flow equation, which is known as Richards' equation:

$$C(h)\frac{\partial h}{\partial t} = \frac{\partial}{\partial z}\left[K(h)\left(\frac{\partial h}{\partial z}+1\right)\right] - S_{\mathrm{a}}(z) \tag{4.8}$$

where $C(h) = \partial\theta/\partial h$ is differential water capacity (cm^{-1}).

SWAP solves the Richards' equation numerically for specified boundary conditions and with know relations between the soil variables θ, h and K. The relation between θ and h (retention function) might be described with the analytical equation proposed by *Van Genuchten* (1980):

$$\theta(h) = \theta_{\mathrm{res}} + \frac{\theta_{\mathrm{sat}} - \theta_{\mathrm{res}}}{\left[1+|\alpha h|^n\right]^{\frac{n-1}{n}}} \tag{4.9}$$

where θ_{res} is residual water content ($cm^3\ cm^{-3}$), θ_{sat} is saturated water content ($cm^3\ cm^{-3}$), and α (cm^{-1}) and n (-) are empirical shape factors. Equation 5.9 in combination with the theory of *Mualem* (1976) provides a versatile relation between θ and K:

$$K(\theta) = K_{\mathrm{sat}} S_{\mathrm{e}}^{\lambda}\left[1-\left(1-S_{\mathrm{e}}^{\,n/n-1}\right)^{\frac{n-1}{n}}\right]^2 \tag{4.10}$$

where K_{sat} is the saturated hydraulic conductivity (cm d^{-1}), λ is an empirical coefficient (-), and S_e is the relative saturation $(\theta - \theta_{res}) / (\theta_{sat} - \theta_{res})$.

4.2.3 Top boundary condition

The top boundary condition is determined by the potential evapotranspiration, irrigation and precipitation fluxes. The potential evapotranspiration can be estimated by the Penman-Monteith equation (*Monteith*, 1965, 1981; *Smith*, 1992; *Allen et al.*, 1998):

$$ET_{\mathrm{p}} = \frac{\frac{\Delta_{\mathrm{v}}}{\lambda_{\mathrm{w}}}\left(R_{\mathrm{n}} - G\right) + \frac{p_1\rho_{\mathrm{air}}C_{\mathrm{air}}}{\lambda_{\mathrm{w}}}\frac{e_{\mathrm{sat}} - e_{\mathrm{a}}}{r_{\mathrm{air}}}}{\Delta_{\mathrm{v}} + \gamma_{\mathrm{air}}\left(1+\frac{r_{\mathrm{crop}}}{r_{\mathrm{air}}}\right)} \tag{4.11}$$

where ET_p is the potential transpiration rate of the canopy (mm d^{-1}), Δ_v is the slope of the vapour pressure curve (kPa K^{-1}), λ_w is the latent heat of vaporization (J kg^{-1}), R_n is the net radiation flux density above the canopy (J $m^{-2}\ d^{-1}$), G is the soil heat flux density (J $m^{-2}\ d^{-1}$), P_1 accounts for unit conversion (= 86400 s d^{-1}), ρ_{air} is the air density (kg m^{-3}), C_{air} is the heat capacity of moist air (J $kg^{-1}\ K^{-1}$), e_{sat} is the saturation vapour pressure (kPa), e_a is the actual vapour pressure (kPa), r_{air} is the aerodynamic resistance (s m^{-1}), γ_{air} is the psychrometric constant (kPa K^{-1}), and r_{crop} is the crop resistance (s m^{-1}). In order to solve Eq. 4.11 the weather variables solar radiation, air humidity, wind speed and air temperature are required. In addition the crop characteristics minimum resistance, reflectance (albedo), and height are needed (*Allen et al.*, 1998).

At a crop which partly covers the soil, ET_p is split into potential soil evaporation E_p (cm d^{-1}) and potential transpiration T_p (cm d^{-1}). This partitioning is achieved by crop leaf area index, *LAI* (-), which is a function of crop development stage (*Goudriaan*, 1977; *Belmans*, 1983):

$$E_p = ET_p e^{-k_{gr} LAI} \tag{4.12}$$

where K_{gr} (-) is the extinction coefficient for global solar radiation. In wet soil conditions, the actual soil evaporation rate E_a (cm d^{-1}) will be equal to E_p. In dry soils conditions, E_a is governed by maximum soil water flux, E_{max} (cm d^{-1}) in top soils, which can be determined by Darcy's law as:

$$E_{\max} = k_{½} \left(\frac{h_{\text{atm}} - h_1 - z_1}{z_1} \right) \tag{4.13}$$

where $k_{½}$ (LT^{-1}) is mean hydraulic conductivity between the soil surface and first node, h_{atm} (cm) is soil water pressure head in equilibrium with the air humidity, h_1 (cm) is the soil water pressure head of first node, and z_1 (cm) is the soil depth of the first node. In our experience the Darcy flux of Eq. 4.13 overestimates the actual soil evaporation flux. Therefore in addition to Eq. 4.13 we used the empirical function of *Black et al.* (1969) to limit the soil evaporation flux to E_{emp}. In our analysis SWAP determined actual evaporation rate by taking the minimum value of E_p, E_{max} and E_{emp}.

The potential transpiration rate, T_p (LT^{-1}), follows from the balance:

$$T_p = \left(1 - \frac{P_i}{ET_{p0}} \right) ET_p - E_p \tag{4.14}$$

where P_i (cm d^{-1}) is the water intercepted by vegetation and ET_{p0} is the potential evapotranspiration of a wet crop, which can be estimated by the Penman-Monteith equation assuming zero crop resistance. The ratio P_i / ET_{p0} denotes the day fraction during which interception water evaporates and transpiration is negligable.

For practical reasons we adopted an homogenous root distribution over the rooting depth. The maximum root water extraction rate S_{max} (d^{-1}) was calculated as:

$$S_{\max} = \frac{T_p}{z_{\text{root}}} \tag{4.15}$$

with z_{root} the rooting depth (cm). Under non-optimal conditions i.e. either too dry, too wet or too saline, S_{max} is reduced. For water stress *Feddes et al.* (1978) proposed a reduction function as depicted in Fig. 4.2. The critical pressure head h_3 for too dry conditions depends on T_p. The values of the input variables h_1, h_2, h_{3h}, h_{3l}, and h_4 (cm) are assumed to be crop specific and can be found in literature (*Taylor and Ashcroft*, 1972; *Doorenbos and Kassam*, 1979; *Wesseling et al.*, 1991; *Smith*, 1992).

The reduction in crop yields due to salinity stress is linearly related to the soil water electrical conductivity *EC* (*Maas and Hoffman*, 1977). Assuming a one to one relationship between relative yield and relative transpiration (Eq. 4.2), they proposed the reduction function depicted in Fig. 4.3.

In case of simultaneous water and salt stress, the actual root water extraction rate S_a (z) is calculated as the product of the reduction coefficients (*Cardon and Letey*, 1992):

$$S_a(z) = \alpha_{rw}\alpha_{rs}S_{max}(z) \qquad (4.16)$$

where α_{rw} and α_{rs} are reduction coefficients (-) for water and salinity stress. The actual transpiration rate T_a follows from the integration of $S_a(z)$ over the rooting depth.

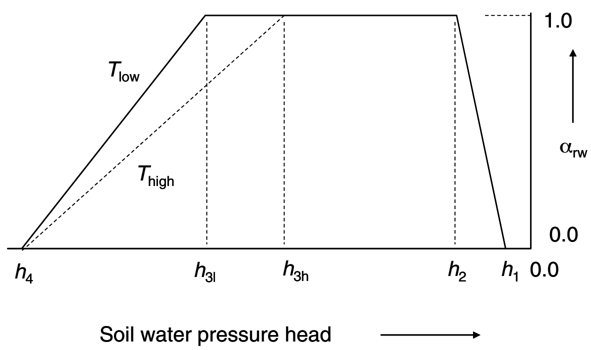

Figure 4.2 Reduction coefficient α_{rw} as function of soil water pressure head *h* and potential transpiration rate T_p (*Feddes et al.*, 1978).

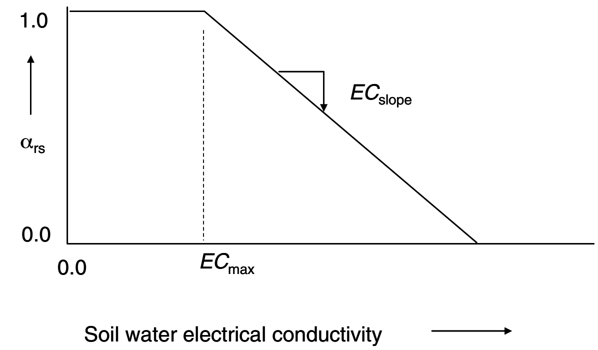

Figure 4.3 Reduction coefficient α_{rs} as function of soil water electrical conductivity EC (*Maas and Hoffman*, 1977).

4.2.4 Bottom boundary condition

In case of deep groundwater levels (< 3 m below soil surface) we will assume free drainage conditions. In that case the percolation flux at the bottom of the soil column will be calculated from:

$$q = -K(h)\left(\frac{\partial h}{\partial z}+1\right) = -k(h)(0+1) = -k(h) \qquad (4.17)$$

In case of shallow groundwater levels (within 3 m of soil surface) the measured groundwater levels were specified as bottom boundary condtion.

4.2.5 Solute transport

The movement of salts in a soil column is governed by convection, diffusion and dispersion. Convection is the bulk movement of salts along with the soil water, diffusion is the net transport of dissolved molecules due to concentration differences, and dispersion is the salt spreading due to different soil water velocities in the soil matrix. In irrigated field soils we may neglect diffusion, as this process is much slower than dispersion. Therefore we described the total salt flux density, J (g cm^{-2} d^{-1}), with:

$$J = J_{con} + J_{dis} \qquad (4.18)$$

where J_{con} is the convection flux density (g cm^{-2} d^{-1}) and J_{dis} is the dispersion flux density (g cm^{-2} d^{-1}). The convection flux follows straight from the soil water flux density q:

$$J_{con} = qC \qquad (4.19)$$

At laminair flux conditions, the dispersion flux density is proportional to the salt concentration gradient and water flux density (*Bear*, 1972):

$$J_{dis} = -q\,L_{dis}\frac{\partial C}{\partial z} \qquad (4.20)$$

where L_{dis} (cm) is the so-called dispersion length.

The principle of salt mass conservation gives for an elementary soil volume:

$$\frac{\partial \theta C}{\partial t} = -\frac{\partial J}{\partial z} \tag{4.21}$$

In Eq. 4.21 decomposition and root uptake of salts are neglected as we are dealing with long term effects in saline soils. Combination of Eqs. 4.18 – 4.21 results in the much applied convection-dispersion equation:

$$\frac{\partial \theta C}{\partial t} = \frac{\partial}{\partial z}\left[q\, L_{\text{dis}} \frac{\partial C}{\partial z} \right] - \frac{\partial q C}{\partial z} \tag{4.22}$$

Equation 4.22 is valid for dynamic, one-dimensional, convective-dispersive salt transport and permits the simulation of root water uptake reduction due to salt stress in the unsaturated/saturated soils (*Jury et al.*, 1991). SWAP solves this transport equation numerically, using specified initial concentrations and concentrations in irrigation and groundwater.

4.3 Materials and methods

4.3.1 Monitoring of farmer fields

Farmer fields were monitored at 6 sites (4 farmer fields at each site) from november 2001 until november 2002. At each site one field was intensively monitored in terms of irrigation supply, crop growth, soil moisture and salinity profiles. The other 3 fields at each site were monitored more extensively and allowed for additional verification. The sites were selected by CCS HAU to have different combinations of crop, water, soil and groundwater conditions. Chapter 3 describes in more detail the sites and measurements program.

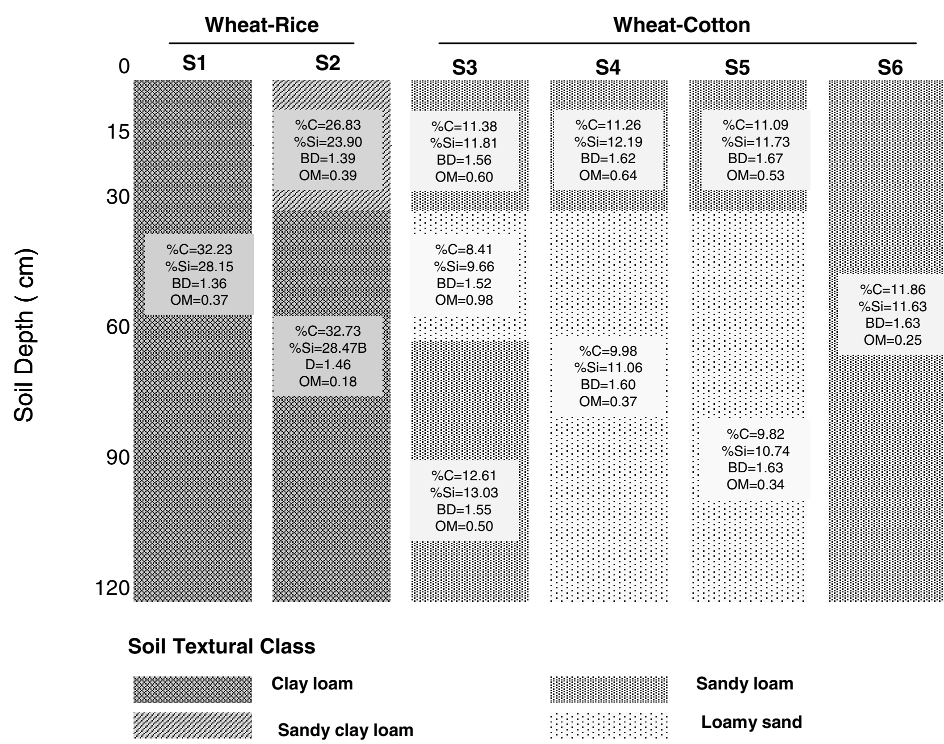

Figure 4.4 Soil texture data at farmer's fields. C = clay, Si = silt, BD = bulk density (g/cm^3) and OM = soil organic matter.

Figure 4.4 shows the soil textures at the 6 sites. The textures range from clay loam to loamy sand. Wheat-rice (sites S1 and S2) is cultivated on heavy soils in a relatively small area. Wheat-cotton, which is predominant in SIC, is mainly cultivated on relatively light soils. The groundwater quality of the wheat-rice region is very good (< 2 dS/m). This is caused by recharge from the seasonally flowing Ghaggar river. In wheat-cotton regions, the groundwater quality varies from good (< 2 dS/m, sites S4 and S5) to marginal (2-4 dS/m, site S3). Site S6 with a wheat-cotton rotation has a small groundwater depth (< 1.5 m) and poor groundwater quality (> 6 dS/m).

The meteorological data of year 2001-02, including minimum and maximum temperature, relative humidity, vapour pressure in the morning and evening, sunshine hours, wind speed and rainfall were collected from a meteorological station installed at ICAR-Cotton Research Institute in Sirsa. The monitored farmers fields were in a range of 20-35 kms from the meteorological station. Plant height, leaf area index, rooting depth, and amounts of dry matter, grain and straw, were recorded during crop development and at the harvest. With respect to irrigation water, the source (canal or tubewell), amount and quality of each irrigation gift were recorded. At the 8 farmer fields in the wheat-rice area hardly canal water was used (<1%). At the 16 wheat-cotton fields the percentage of canal water ranged from 30 % (site S3) to 60 % (S5), with a maximum (90 %) at site S6 with poor groundwater quality.

4.3.2 Input parameters of SWAP

The SWAP input parameters might be categorized into atmosphere, crop, water and soil. Most of the information required for the application of SWAP could be measured directly in the fields or laboratory. Note that in this chapter the crop development (*LAI*, rooting depth) is prescribed according to the measurement data.

The upper boundary was defined by the potential evapotranspiration and amounts of rainfall and irrigation. For this study, potential evapotranspiration was estimated by the Penman-Monteith equation (Eq 5.11) using recorded meteorological data. Most of the parameters used by Eq. 4.11 can be calculated from standard meteorological data and crop parameters measured at fields (Allen et al., 1998). The meteorological data obtained from ICAR-Cotton Research Institute, Sirsa were not accurate enough. Therefore, a comparison with data from a metorological station of HAU at Hisar (about 90 km from Sirsa) was made, and if needed corrections were made (see attached CD-ROM).

The observed leaf area index was used for partitioning of potential evapotranspiration into potential soil evaporation and potential transpiration. In addition to the maximum Darcy flux, the empirical equation of *Black et al.* (1969) was used to restrict actual soil evaporation. The plant height, leaf area index, and rooting depth were prescribed according to the measurements as function of crop development stage. The critical pressure head values for root water uptake were derived from literature. For salt transport the dispersion length L_{dis} was set to 5 cm (*Nielsen et al.*, 1986). The various input parameters are summarized in Table 4.1.

Table 4.1 **Input parameters as used in SWAP at the farmer fields.**

Parameter	Wheat	Rice	Cotton
Evaporation			
Evaporation coefficient of Black (cm $d^{-½}$)	0.35	-	0.35
Crop			
Minimum canopy resistance, r_{crop} (s m^{-1})	70	70	70
Critical pressure heads, h (cm)			
h_1	-1.0	100.0	-1.0
h_2	-22.9	55.0	-22.9
h_{3l}	-1000	-160	-1200
h_{3h}	-2200	-250	-7500
h_4	-16000	-16000	-16000
Light extinction coefficient, K_{gr}	0.375	0.300	0.450
Salinity			
Critical level, EC_{max} (dS/m)	6.0	3.0	7.7
Decline per unit EC, EC_{slope} $(dS/m)^{-1}$	7.1	11.1	5.4
Dispersion length, L_{dis} (cm)	5.0	5.0	5.0

The initial soil moisture was not measured at all fields; therefore, the initial moisture profile was generated by running SWAP one year in advance and using the final pressure heads as initial condition. The initial salinity profile was derived from the field measurements.

4.3.3 Inverse modeling of soil hydraulic functions

Water flow and salt transport is very sensitive to the soil hydraulic functions $\theta(h)$ and $K(\theta)$. The parameters describing these functions (Eqs. 4.9 and 4.10) were based on the measured texture and so-called PedoTransfer Functions (PTF) which relate soil texture with $\theta(h)$ and $K(\theta)$. However the accuracy of PTF is limited for site specific water flow and salt transport. Therefore the soil hydraulic parameters had be calibrated either manually or automatically. We used automatic calibration, which is also called inverse modeling.

At each site the measured soil moisture and salinity profiles before and after irrigation in *rabi* were used for the calibration of the soil hydraulic functions. A non-linear parameter estimation program, PEST (*Doherthy et al.*, 1995) was linked with SWAP (Fig. 4.5). An objective function quantifies the differences between model results and observations. If the observation error follow a multivariate normal distribution with zero mean, no correlation, and constant variance for each measurement type, maximization of the probability of reproducing the observed data leads to the weighted least squares objective function $O(\mathbf{b})$:

$$O(\mathbf{b}) = \sum_{i=1}^{N} \left[\left\{ w_\theta \left(\theta_m(t_i) - \theta(\mathbf{b}, t_i) \right) \right\}^2 + \left\{ w_{EC} \left(EC_m(t_i) - EC(\mathbf{b}, t_i) \right) \right\}^2 \right] \quad (4.23)$$

where $\theta_m(t_i)$ and $EC_m(t_i)$ are the observed soil moisture and soil salinity at time t_i, N is the number of measurements, $\theta(\boldsymbol{b},t_i)$ and $EC(\boldsymbol{b},t_i)$ are the simulated values of θ and EC using an array with parameter values $\boldsymbol{b}$, and w_θ and w_{EC} are weighting factors. In case of random observation errors only, according to maximum likelihood the weighting factor for a particular observation should be equal to the inverse of the standard deviation of the observation error of that particular observation type. *Gribb* (1996) weighted each different data type by the inverse of the mean values. We used w_θ = 1 and w_{EC} = 10% of average measured water content divided by average measured salinity concentration. In this way we accounted for measurement unit differences of θ and *EC* and at the same time gave relatively more weight to the water content measurents.

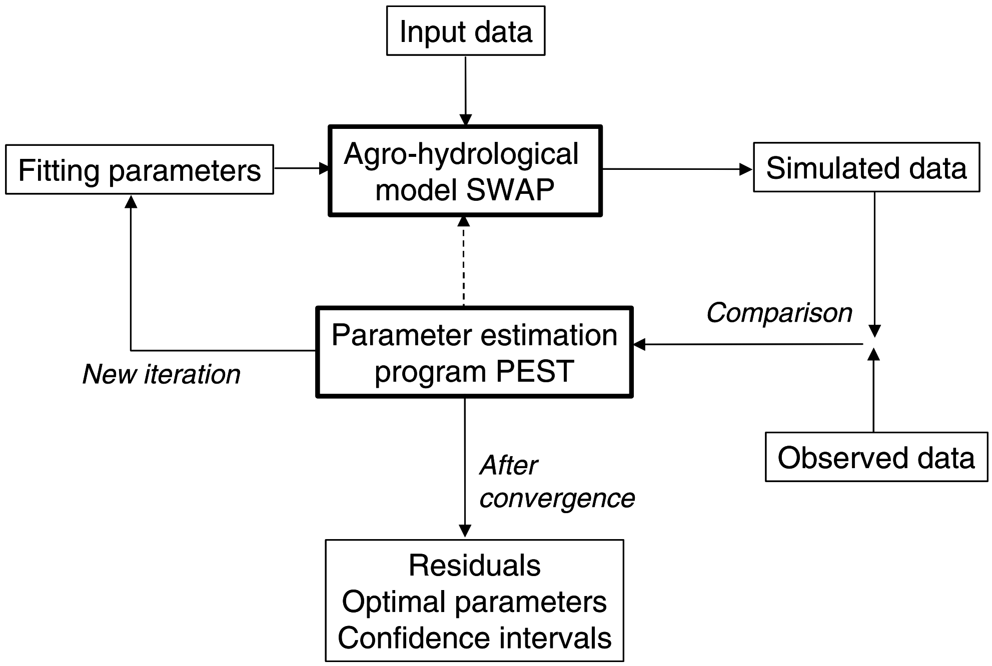

Figure 4.5 Communication between simulation model SWAP and parameter estimation program PEST.

A standard inverse method must be well-posed in order to achieve unique and stable parameter estimates. A well-posed inverse problem can be realized by reducing the number of fitting parameters (*Kool and Parker,* 1988). Of the parameters describing the soil hydraulic functions (Eqs. 4.9 and 4.10) the saturated soil moisture content, θ_s (cm^3cm^{-3}) and saturated hydraulic conductivity, K_{sat} (cm/day) have a clear physical meaning, and can be measured easily. So the values of these parameters were taken from the measurements at various fields. The residual water content θ_r (cm^3cm^{-3}) and the shape parameter λ show low sensitivity and were derived from pedotransfer functions (*Russo*, 1988). Two soil hydraulic parameters remained uncertain: α (cm^{-1}) and *n*. Most of the fields considered in this study have two or three soil layers (Fig. 4.4), the total number of fitting parameters therefore amounted 4-6. In case of regular measurements at ordinary field conditions, 4-8 hydrological parameters could be estimated uniquely with a low coefficient of correlation and variation (*van Dam*, 2000). Pedotransfer functions were used to derive initial estimates of the fitting parameters.

4.3.4 Water Management Response Indicators

High crop yields indicate the success or failure of irrigation and drainage, but they provide no information on the environmental sustainability or the difference between intended and actual water deliveries of an irrigation system (*Molden and Gates*, 1990). The goals of efficient water management are to achieve maximum crop yields with a minimum amount of water along with sustainability ensuring control of waterlogging, salinization and environmental degradation. Water Management Response Indicators (WMRI) quantify the realization of these goals (*Bastiaanssen* et al., 1996).

We used the WMRI's as listed in Box 4.1. Relative transpiration gives actual crop water use and is directly related to the crop yield (Eq. 4.2). This ratio indicates the intensity of water and salt stress on the crop. The contribution of different water resources to actual evapotranspiration is quantified by the rainfall and irrigation contribution index. The percolation index indicates the leaching fraction and therefore the salinization or waterlogging risk. The salt storage index expresses the salt build up in the root zone. For a sustainable system, the salt storage change must be near zero or negative over a long period.

Box 4.1 Definiton of Water Management Response Indicators (Bastiaanssen et al., 1996)

Relative transpiration $= \dfrac{T_a}{T_p}$

Rainfall contribution $= \dfrac{P}{ET_a}$

Irrigation contribution $= \dfrac{I}{ET_a}$

Percolation index $= \dfrac{Q_{bot}}{I}$

Salt storage index $= \dfrac{\Delta C}{C}$

with T_a and T_p the actual and potential transpiration (mm), ET_a is the actual evapotranspiration (mm), P and I are rainfall and irrigation water amounts (mm), Q_{bot} is deep percolation (mm, + upward), and C and ΔC (g cm^{-3}) are the initial and change in salt storage in the soil profile.

4.4 Results and discussion

4.4.1 Soil hydraulic functions

Soil moisture and salinity profiles were measured during the entire crop growing period (January-April). The calibration process was performed with the first part of the observations, and the second part of the observations was used for validation. The soil hydraulic parameters α and n of the different soil layers of the stratified soil profile were optimized simultaneously. Table 4.2 shows the optimized parameter values together with the other soil hydraulic parameter.

Table 4.2 Derived soil hydraulic parameters at the 6 measurement sites. Parameters α and n are optimized.

Field	Soil Layer (cm)	Texture	Soil hydraulic parameters					
			θ_r (cm^{3}cm^{-3})	θ_s (cm^{3}cm^{-3})	K_{sat} (cm d^{-1})	α (cm^{-1})	λ (-)	n (-)
			Wheat-Rice combination					
S1F1	>0	CL	0.01	0.57	1.57	0.005	-2.57	1.93
S2F5	0-30	SiCL	0.01	0.50	2.63	0.010	-2.53	1.40
	>30	CL	0.01	0.58	1.87	0.005	-2.37	1.77
			Wheat-Cotton combination					
S3F11	0-30	SL	0.01	0.34	61.82	0.011	-1.55	1.42
	30-60	LS	0.01	0.33	73.81	0.052	-1.35	1.19
	>60	SL	0.01	0.38	60.58	0.005	-1.58	1.58
S4F16	0-30	SL	0.01	0.31	101.71	0.014	-1.67	1.29
	>30	LS	0.01	0.32	120.87	0.036	-0.87	1.19
S5F20	0-30	SL	0.01	0.34	138.69	0.041	-1.56	1.21
	>30	LS	0.01	0.31	141.62	0.024	-0.80	1.16
S6F24	>0	SL	0.01	0.36	132.82	0.080	-0.91	1.19

Repetition of the optimisation process with different initial parameter values resulted in the same results which showed the uniqueness of the solution. Table 4.3 lists the coefficient of variation (ratio of standard deviation and mean) and the correlation between the parameters. The coefficient of variation was relatively low for the parameter *n* compared to the parameter α. This is attributed to the higher sensitivity of parameter *n* to soil moisture flow (*Ritter et al.*, 2003). For proper calibration also the correlation coefficients of the estimated parameters should be small. As Table 4.3 shows, the correlation coeffcients were acceptably small.

Table 4.3 Coefficients of variation and correlation matrix of optimized parameters for two typical examples: fields S1F5 and S5F20.

Soil layer (cm)	Parameter	Optimized value	Coefficient of variation	Correlation coefficient			
				α_1	n_1	α_2	n_2
		Field S2F5	(Wheat-Rice combination)				
30	α_1	0.010	0.271	1.000			
	n_1	1.40	0.064	0.153	1.000		
>30	α_2	0.005	0.504	0.594	0.864	1.000	
	n_2	1.77	0.021	0.255	0.380	0.425	1.000
		Field S5F20	(Wheat-Cotton combination)				
30	α_1	0.041	1.474	1.000			
	n_1	1.20	0.100	-0.771	1.000		
>30	α_2	0.024	1.182	0.530	0.122	1.000	
	n_2	1.16	0.010	0.228	-0.093	0.256	1.000

As a typical example Fig. 4.6 shows the observed and simulated water contents and salinity concentrations of field S5F20. The average *RMSE* of θ and *EC* of this field were 0.022 (cm^3cm^{-3}) and 0.08 (dS/m) in the wheat season, showing that soil water flow and salt transport were well simulated by SWAP. A slightly higher *RMSE* value (0.051 cm^3cm^{-3}) of θ during the cotton crop was caused by some overestimation of soil moisture, particularly at deeper soil depths (Fig. 4.6). This might be caused by the spatial variation of rainfall during the monsoon season.

Table 4.4 Numer of observations *N* and *RMSE* of soil moisture and salinity for both the calibration period (first part wheat season) and validation period (second part wheat season).

Field No.	Calibration				Validation			
	θ (cm^3cm^{-3})		*EC* (dS/m)		θ (cm^3cm^{-3})		*EC* (dS/m)	
	N	*RMSE*	*N*	*RMSE*	*N*	*RMSE*	*N*	*RMSE*
S1F1	15	0.032	10	0.179	13	0.023	15	0.195
S2F5	15	0.016	15	0.201	15	0.027	15	0.247
S3F11	20	0.025	20	0.254	20	0.033	20	0.308
S4F16	25	0.022	25	0.147	20	0.026	20	0.102
S5F20	30	0.022	25	0.094	30	0.022	25	0.067
S6F24	18	0.037	15	1.289	20	0.039	15	1.839

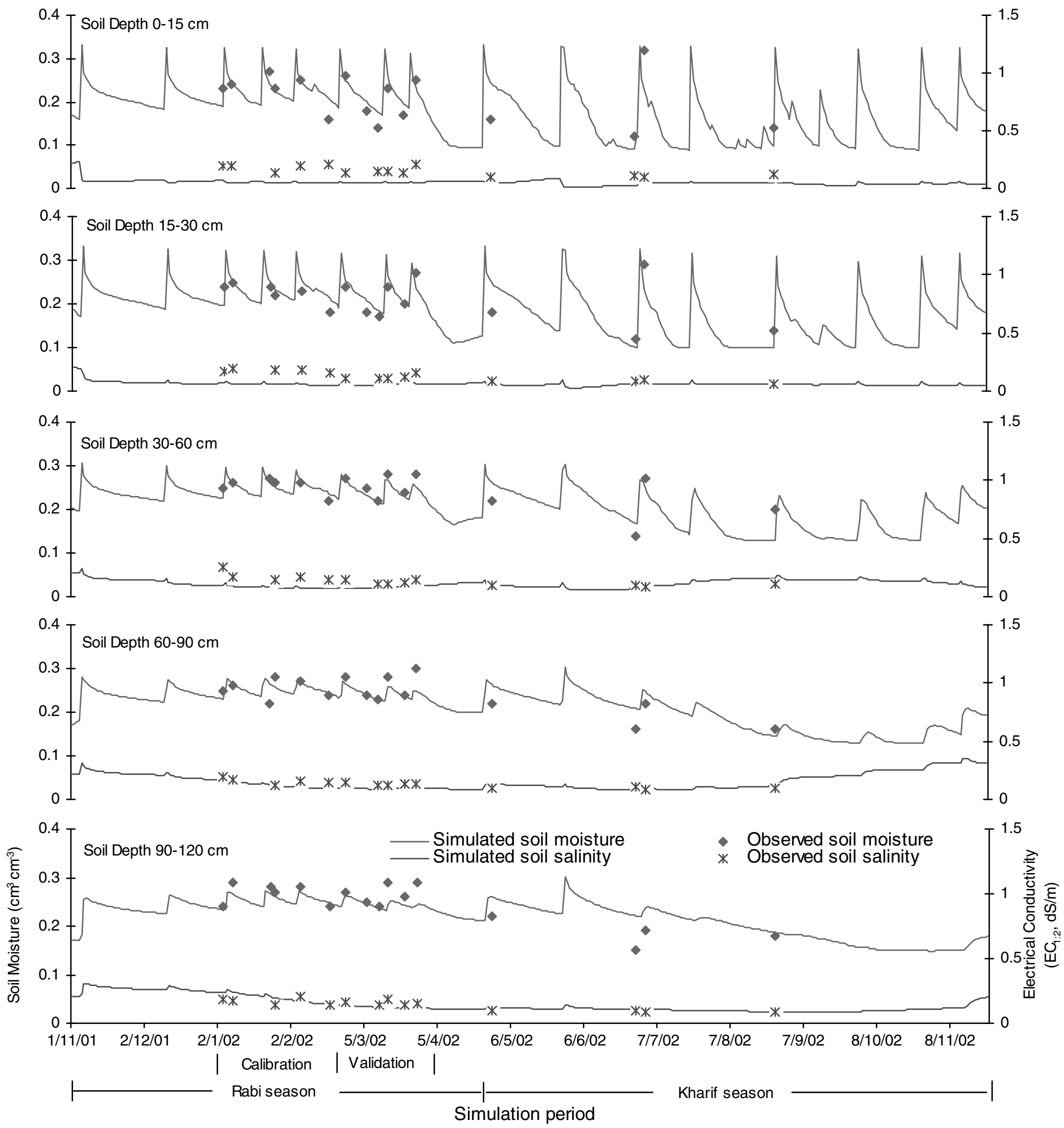

Figure 4.6 Typical example (field S5F20 with wheat-cotton rotation) of observed and simulated soil moisture and salinity concentrations. Calibration was performed for the first half of the *rabi* season.

The Root Mean Square Error (*RMSE*) is useful to quantify the differences between observed data and simulated data with the optimized parameters:

$$RMSE = \sqrt{\frac{1}{N}\sum_{i=1}^{N}\left[M_i - S_i(\mathbf{b})\right]^2} \quad (4.24)$$

where M_i and S_i ($\boldsymbol{b}$) are measured and simulated values for an output variable. Table 4.4 lists the *RMSE* values in case of θ and *EC* values in the soil profile. The *RMSE* of θ (cm^3cm^{-3}) ranges from 0.016 to 0.039. These small values reveal a good to acceptable calibration and validation of the model at all fields. The simulation of *EC* was also in good agreement with observations at all fields, except at field S6F24 (*RMSE* = 1.839 dS/m) which has a shallow water table with poor groundwater quality. As no systematic under- or overestimation of θ and *EC* was observed, the differences in simulated and observed θ and *EC* are contributed to spatial variation and observation errors which are inevitable at field conditions.

4.4.2 Water and salt balances

Wheat-cotton and wheat-rice are the most prominent crop rotations in SIC. Wheat is the main crop during the *rabi* season and cotton/rice during the *kharif* season. Early sowing (in October) of wheat is practised in wheat-rice regions, while late sowing (in November) is practised in wheat-cotton regions. In 2002 the sowing of *kharif* crops was delayed 15-20 days due to a late start of the monsoon. The late sowing of *kharif* crops resulted in late harvesting. The period 1 Nov 2001 – 31 Oct 2002 was comparatively dry with a total rainfall amount of 190 mm as compared to 370 mm in an average year. The calibrated soil hydraulic parameters (Table 4.2) along with other inputs (Table 4.1) were used to simulate the water and salt balances of the farmer fields at the 6 investigated sites.

Wheat-Cotton combination

The water and salt balances for *rabi* (1 Nov 2001 – 30 Apr 2002) and *kharif* (1 May 2002 – 20 Nov 2002) for wheat-cotton are presented in Table 4.5. The average annual ET_p for the wheat-cotton combination according to the Penman-Monteith equation (Eq 4.11) was as high as 2097 mm. A relative transpiration T_a / T_p = 0.75 is acceptable for Haryana conditions (*Boumans et al.*, 1988). The relative transpiration was sufficiently high (> 0.75) for wheat crop at all fields, except at S6F24 where a very high salt stress was observed (T_a / T_p = 0.66). We also simulated field S6F24 without salt stress. In that case T_a / T_p would rise from 0.66 to 0.96 for wheat and from 0.37 to 0.55 for cotton. This shows the relative impacts of salt stress and water stress in both seasons. The average ET_p during *kharif* season (≈1500 mm) was 2.5 times higher than *rabi* season (≈ 580 mm), while the relative irrigation supplies were more during *rabi* season (Table 4.5). The cotton crop at all fields was under water stress showing a lower value (≈ 0.60) of relative transpiration. Main causes are irrigation water shortage and the low rainfall (≈ 180 mm) in the monsoon of 2002.

Table 4.5 Computed seasonal water and salt balance components for the wheat-cotton rotation.

Field	Crop season	Water balance components (mm)							
		P	I	T_p	T_a	E_p	E_a	Q_{bot}	ΔW
S3F11	*Rabi* (wheat)	11	430	275	244	313	94	-77	23
	Kharif (cotton)	177	301	438	277	899	151	-86	-37
S4F16	*Rabi* (wheat)	11	391	299	253	303	99	-6	42
	Kharif (cotton)	177	554	909	582	617	164	-25	-44
S5F20	*Rabi* (wheat)	11	568	253	245	305	111	-171	52
	Kharif (cotton)	177	737	1054	685	623	142	-132	-51
S6F24	*Rabi* (wheat)	11	336	192	126	387	81	-151	-11
	Kharif (cotton)	177	285	922	339	604	102	-19	-6
		Salt balance components (mg cm^{-2})(1)							
			IC_i					$Q_{bot}C_{bot}$	ΔC
S3F11	*Rabi* (wheat)		102					-19	83
	Kharif (cotton)		33					-22	11
S4F16	*Rabi* (wheat)		25					-3	22
	Kharif (cotton)		36					-11	24
S5F20	*Rabi* (wheat)		20					-49	-30
	Kharif (cotton)		26					-38	-12
S6F24	*Rabi* (wheat)		13					-412	-400
	Kharif (cotton)		5					-276	-270

(1) Height soil column considered is 300 cm.

Potential transpiration for wheat ranged from 192 mm at field S6F24 (Table 4.5) in saline and waterlogged area to 364 mm at field S1F1 (Table 4.7) in the well-productive wheat-rice region. Similarly, for cotton T_p ranged from 438 to 1054 mm (Table 4.5). The actual annual evapotranspiration, ET_a for wheat-cotton estimated by SWAP ranged from 648 mm in shallow watertable and saline (field S6F24) region to 1182 mm in the well-productive (S5F20) areas. The comparative crop performance on different fields was evaluated by the relative transpiration. As T_p we used the potential transpiration of the best developed crops (in case of wheat 364 mm at field S1F1 and in case of cotton 1054 mm at field S5F20). Table 4.6. shows that the actual crop yields are ≈68 and 60% of potential yields for wheat and cotton, respectively, in fresh groundwater areas, while only ≈ 35% (S6F24) in saline and waterlogged areas.

Table 4.6 Computed annual water management response indicators (Box 4.1) for the wheat-cotton rotation.

Field	Water Management Response Indicators						
	Relative transpiration		Rainfall contribution	Irrigation contribution		Percolation index	Salt storage index
	Wheat	Cotton		Canal	Tubewell		
S3F11	0.67	0.26	0.24	0.28	0.68	-0.22	1.32
S4F16	0.69	0.55	0.17	0.00	0.86	-0.03	0.21
S5F20	0.67	0.65	0.16	0.00	1.10	-0.23	-0.26
S6F24	0.35	0.32	0.29	0.78	0.18	-0.27	-0.25

Table 4.6 shows the WMRI for the wheat-cotton rotation. The annual percolation index was < -0.20 for most of the fields, except at field S4F16. In this field the perolation index of -0.03 indicates salt buildup in the soil profile, which is also clear from the salt storage index. The salt storage index was also relatively high for field S3F11 despite a percolation index of -0.22. This is caused by the poor groundwater quality (3.73 dS/m) at this field.

The rainfall contribution to crop evapotranspiration was mainly during *kharif* (cotton), and very low (≈190 mm) as compared to irrigation supplies to the fields. The tubewell water amounts compared to canal irrigation amounts were very high at most of the fields, except field S6F24. The low canal water supplies are attributed to the low rainfall and drought conditions throughout the agricultural year 2001-02. The high canal water contribution in the saline region (S6F24) must be due to restriction on groundwater use. The use of more canal water in saline region is beneficial in leaching of salt (salt storage index = -0.25), but also contributes to more recharge (percolation index = -0.27), which may increase waterlogging and secondary salinization in the future.

Wheat-Rice combination

For optimal growing conditions of rice, farmers maintain water ponding on the soil surface during the rice season. In order to reduce the seepage losses, the soil is puddled before rice transplantation. In the simulation of soil water flow during rice crop, therefore the saturated hydraulic conductivity of the upper 30 cm soil depth was reduced to 20 % in order to capture the effect of soil puddling.

The water and salt balance for *rabi* (1 Oct 2001 - 30 April 2002) and *kharif* (1 May 2002 – 15 Oct 2002) for wheat-rice is presented in Table 4.7. The simulated annual ET_p for wheat-rice was 1963 and 2021 mm at field S1F1 and S2F5, respectively. The actual evapotranspiration, ET_a for individual wheat and rice crops was 411 and 880 mm, respectively. This gives an annual ET_a of 1291 mm in case of the wheat-rice rotation, while ET_a amounted 1349 mm in case of the wheat-cotton rotation. The high value of average E_a (415 mm) during the rice season as compared to 94 mm during the wheat season were due to water ponding on the soil surface in the rice crop.

Table 4.7 Computed seasonal water and salt balance components for the wheat-rice crop rotation.

Field	Crop season	Water balance components (mm)							
		P	I	T_p	T_a	E_p	E_a	Q_{bot}	ΔW
S1F1	*Rabi* (wheat)	13	343	364	364	353	88	-329	-43
	Kharif (rice)	177	1250	475	457	772	405	-121	44
S2F5	*Rabi* (wheat)	13	424	330	326	381	99	-195	-19
	Kharif (rice)	177	1062	565	536	744	425	-98	18
		Salt balance components (mg cm^{-2})(1)							
			IC_i					$Q_{bot}C_{bot}$	ΔC
S1F1	*Rabi* (wheat)		20					-31	-11
	Kharif (rice)		74					-11	63
S2F5	*Rabi* (wheat)		24					-75	-51
	Kharif (rice)		61					-41	20

(1) Height soil column considered is 300 cm.

The soil water storage decreased during the wheat crop and increased during the rice crop. The higher percolation (-329 and -195 mm) during wheat season is attributed to the saturated soil profile left after rice crop and heavy irrigations of ≈ 200 mm in the early stage (Oct-Nov) of the wheat crop. However, large irrigations (≈1150 mm) during *kharif* season produces less percolation because the creation of a puddled soil layer (low saturated hydraulic conductivity) before rice transplantation results in water ponding. The table shows the leaching of salt during the wheat season (ΔC = negative), and salt accumulation in the rice season (ΔC = positive).

Table 4.8 lists the WMRI of the wheat-rice rotation. The relative transpiration was relatively high (> 0.75) due to high irrigation (≈ 1540 mm) supplies. The relative transpiration showed that actual yields for wheat and rice are very close to the potential yields. The average observed yields of 6.5 and 7.7 t/ha for wheat and rice at fields S1F1 and S2F5 confirmed a very good crop growth in the wheat-rice regions which has a good groundwater quality. The annual salt storage index at field S1F1 showed salt build up in soil profile having a high value of percolation index (-0.28), while at field S2F5 leaching of salts was observed with a low value of percolation index (-0.20). The positive salt storage index at field S1F1 was caused by very low initial salt concentrations.

Table 4.8 Computed annual water management response indicators (Box 4.1) for the wheat-rice rotation.

Field	Water Management Response Indicators						
	Relative transpiration		Rainfall contribution	Irrigation contribution		Percolation index	Salt storage index
	Wheat	Rice		Canal	Tubewell		
S1F1	1.00	0.81	0.15	0.00	1.21	-0.28	0.44
S2F5	0.90	0.95	0.14	0.00	1.07	-0.20	-0.10

4.5 Soil hydraulic parameters for regional scale

A large region as Sirsa Irrigation Circle might be divided into homogeneous units with respect to soil, landuse, groundwater, etc. The SWAP-WOFOST combination might be applied to each of these units, to derive regional *WP* values (Chapter 7 and 9). In order to do so, for each soil unit the soil hydraulic properties are required. Pedotransfer functions (PTF) might be used to estimate the soil hydraulic properties using soil texture information which is available on regional scale. Nemes et al. (2003) showed the potential of using of internationally developed PTF as an alternative to laboratory measurements. However, they stressed the importance of the testing PTF with the specific model for the specific research goal.

The PTF based on a European soil database (HYPRESS: *Wösten et al*., 1998) was tested at different farmer fields for their suitability to derive *WP* in Sirsa Irrigation Circle. The input soil information (percent clay, silt, organic matter and bulk density) required by HYPRESS to derive the soil hydraulic parameters was extracted from a soil survey in Sirsa by *Ahuja et al*. (2001). Table 4.9 lists the resulting parameters.

Table 4.9 Soil hydraulic parameters derived by pedotransfer functions based on HYPRESS.

Soil texture	Soil layer (cm)	Soil hydraulic parameters					
		θ_r (cm^3 cm^{-3})	θ_s (cm^3 cm^{-3})	K_s (cm d^{-1})	α (cm^{-1})	λ (-)	n (-)
Sandy loam	0-30	0.01	0.36	51.98	0.059	-1.58	1.28
	>30	0.01	0.36	25.16	0.067	-1.43	1.26
Loamy sand	0-30	0.01	0.34	74.93	0.066	-0.63	1.39
	>30	0.01	0.35	36.12	0.088	0.23	1.41

The performance of PTF was compared with the calibrated soil hydraulic parameters at fields in the wheat-cotton region. The initial moisture profile generated during the calibration process was considered as measured. The same initial soil moisture profiles were used for the simulation based on parameters derived by PTF. Table 4.10 shows that in case of PTF the discrepancies in simulated and observed soil moisture were higher, particularly at field S3F11, while salt concentrations were simulated as good as at simulations based on the calibrated soil hydraulic parameters.

Table 4.10 *RMSE* of measured and simulated water contents and *EC* concentrations using calibrated and HYPRESS soil hydraulic parameters.

Field	Calibrated		Pedotransfer function	
	θ (cm^3cm^{-3})	*EC* (dS/m)	θ (cm^3cm^{-3})	*EC* (dS/m)
S3F11	0.029	0.284	0.075	0.193
S4F16	0.025	0.142	0.038	0.131
S5F20	0.022	0.080	0.043	0.079

Table 4.11 Water Management Response Indicators (Box 4.1) as simulated by SWAP using calibrated and HYPRESS soil hydraulic parameters.

Field	Relative transpiration				Percolation index		Salt storage index		Change in water storage (mm)	
	Calibrated		PTF		Calibrated	PTF	Calibrated	PTF	Calibrated	PTF
	Wheat	Cotton	Wheat	Cotton						
S3F11	0.67	0.26	0.73	0.29	-0.22	0.0	1.32	1.89	-14	121
S4F16	0.69	0.55	0.74	0.54	-0.03	-0.13	0.21	0.02	-2	-82
S5F20	0.67	0.65	0.67	0.62	-0.23	-0.33	-0.26	-0.47	-1	-110

The actual evapotranspiration by PTF was found to be fairly close to that estimated by calibrated soil hydraulic parameters (Table 4.11) at all 3 fields. The percolation index and salt storage index were deviating in comparison to those estimated by calibrated soil hydraulic parameters which is mainly caused by the invoked initial conditions. However, the good correspondence for relative transpiration (Table 4.11) shows the potential to use PTF from databases as HYPRESS to derive soil hydraulic parameters for regional water productivity analysis in Sirsa district.

4.6 Conclusions

The good agreement between simulated and observed soil moisture (RMSE ≈ 0.016 to 0.039 cm^3cm^{-3}) and salinity (RMSE ≈ 0.094 to 1.839 dS/m) provides confidence to use the calibrated and validated SWAP model to derive water and salt balances at the different sites for current and optional water management. The inverse methodology was found to be efficient in the calibration of the soil hydraulic parameters using observed soil moisture and salinity before and after irrigation events. The water and salt balance analysis at different fields showed a very high exploitation of groundwater in wheat-rice regions (field S1F1 and S1F5). The use of poor groundwater quality was found to be resulting in high salt buildup ($\Delta C / C_i$ = 1.32 at field S3F11). The water stress was observed more on *kharif* crops i.e. cotton ($T_a / T_p \approx 0.60$) as compared to wheat crop ($T_a / T_p > 0.75$). The crop performance as indicated by relative transpiration was almost potential (≈ 0.90) in wheat-rice regions, while it was very poor (≈ 0.30) in waterlogged and saline conditions (field S6F24).